CO2 Capture by Injection of Flue Gas or CO2−N2 Mixtures into Hydrate Reservoirs: Dependence of CO2 Capture Efficiency on Gas Hydrate Reservoir Conditions

CO_2 Capture by Injection of Flue Gas or CO_2-N_2 Mixtures into Hydrate Reservoirs: Dependence of CO_2 Capture Efficiency on Gas Hydrate Reservoir Conditions

Aliakbar Hassanpouryouzband[1], Jinhai Yang[1*], Bahman Tohidi[1], Evgeny Chuvilin[2], Vladimir Istomin[2], Boris Bukhanov[2], and Alexey Cheremisin[2]

[1] Hydrates, Flow Assurance & Phase Equilibria Research Group, Institute of Petroleum Engineering, Heriot-Watt University, Edinburgh, EH14 4AS, UK.
[2] Skolkovo Institute of Science and Technology, Moscow 143026, Russia

Abstract

Injection of flue gas or CO_2-N_2 mixtures into gas hydrate reservoirs has been considered as a promising option for geological storage of CO_2. However, the thermodynamic process in which the CO_2 present in flue gas or a CO_2-N_2 mixture is captured as hydrate has not been well understood. In this work a series of experiments were conducted to investigate the dependence of CO_2 capture efficiency on reservoir conditions. The CO_2 capture efficiency was investigated at different injection pressures from 2.6 to 23.8 MPa and hydrate reservoir temperatures from 273.2 to 283.2 K in the presence of two different saturations of methane hydrate. The results showed that more than 60% of the CO_2 in the flue gas was captured and stored as CO_2 hydrate or CO_2-mixed hydrates, while methane-rich gas was produced. The efficiency of CO_2 capture depends on the reservoir conditions including temperature, pressure, and hydrate saturation. For a certain reservoir temperature, there is an optimum reservoir pressure at which the maximum amount of CO_2 can be captured from the injected flue gas or CO_2-N_2 mixtures. This finding suggests that it is essential to control the injection pressure to enhance CO_2 capture efficiency by flue gas or CO_2-N_2 mixtures injection.

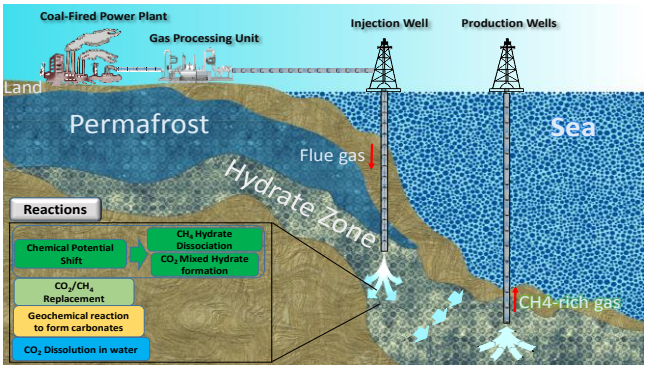

* Corresponding author: petjy@hw.ac.uk (J Yang)

Keywords: Carbon dioxide capture and storage; gas hydrate; flue gas; optimum conditions; carbon dioxide replacement; methane recovery.

1. Introduction

Gas hydrate is a naturally occurring crystalline solid composed of a host lattice of water molecules that encages guest gas molecules without chemical bonding[1]. The principal guest molecule in naturally occurring hydrates is CH_4, very significant volume of which is trapped in natural sediments[2]. Methane hydrate (MH) is known to exist under permafrost, and in continental and margin sediments[3] potentially providing a sustainable energy resource[4] and also powerful reservoirs to mitigate increasing effect of CO_2[5] on the climate, with respect to reduced geological hazards[6] and sufficient energy efficiency[7].

CO_2 as the most important anthropogenic greenhouse gas is responsible for more than half of the increasing greenhouse effect[8]. However, given the existing infrastructure for production, transfer, and utilization, fossil fuels (main source of CO_2 emission) will continue to play a major role in heat and power generations for the predictable future[9]. Accordingly, techniques developed for carbon dioxide capture and storage (CCS) play a crucial role in control of global warming, standing as the major environmental challenge. Despite significant technological advancements in CO_2 storage (CS) techniques, challenges still exist in the development of complex and fully functional methods that can be applied on an industrial scale[10]. To address these challenges, CS in natural MH reservoirs has emerged, which is considered as a promising approach for permanent CS[5]. Furthermore, CO_2 hydrate (CH) is thermodynamically more stable than both MH structure I and II, enabling exothermic[11] replacement of CH_4 with CO_2. CO_2 replacement adds heat to the MH reservoir, increasing the methane production rate[12] and leading to more economic methane production. As a result, injection of CO_2 into MH reservoirs can not only recover methane by CO_2 replacement but also reduce the impact of hydrate dissociation on geomechanical stability of the hydrate deposits due to formation of CO_2 hydrate or CO_2-mixed hydrates. This secondary hydrate formation will also consume the released water and cement the released sands after MH dissociation, results in limiting the migration of water, and sand significantly, when compared with other methane recovery methods[13,14]. However, more thorough investigations are required to quantify this effect. Recent studies have included various approaches towards understanding

54 the CH_4−CO_2 replacement mechanism, including liquid CO_2 injection[15], kinetic study using in situ laser
55 Raman spectroscopy[16], micro differential scanning calorimeter[17], and magnetic resonance imaging[18],
56 and enhanced CH_4−CO_2 replacement in the presence of thermal stimulation[19]. Further information can
57 be found elsewhere[20–22].
58 Despite all of the proposed benefits, CS in hydrate reservoirs has high-cost barriers that prevents its
59 wide deployment[23–25]. In this case, CO_2 capture prior to storage is the major[26,27] cost. It was estimated
60 that the cost of CO_2 separation and disposal from coal-fired power plants can increase the cost of
61 electricity by about 75%[28]; much of this cost (up to 80%[28]) is caused by separation of CO_2, the removal
62 of which leads to an increase in power efficiency from 26% to 38%[29]. In addition, another major energy
63 penalty comes from compression of the flue gas before injection, which should be considered before
64 any field trials. There are extensive efforts associated with improvement of the CO_2 capture efficiency,
65 such as optimizing the capture plant design and capturing parameters, or developing new absorbents,
66 adsorbents, membrane materials[30] whose principal aims are towards a breakthrough in the development
67 of low-cost CO_2 capture technology. However, the predominant obstacles associated with the
68 exploitation of this method, apart from the clear economic challenges, are connected with scaling up in
69 order to encourage public investment[31].
70 Injection of CO_2-N_2 mixtures instead of pure CO_2 into gas hydrate reservoirs could significantly reduce
71 CO_2 separation costs. It was reported that using (N_2+CO_2) gas mixtures improved CO_2-CH_4 exchange
72 rate[6,32,33] and resulted in a higher methane recovery ratio[32] and higher mobility in sediments[34] compared
73 to those of supercritical or pure CO_2. Moreover, an industrial scale test of CO_2 replacement in the North
74 Slope of Alaska has shown that injecting a gas mixture of 23% CO_2 and 77% N_2 into a hydrate layer
75 with simultaneous recovery of methane has proven successful, preventing CO_2 hydrate build-up around
76 the injection well[35]. Overall performance was also excellent and incident-free, which is a very positive
77 sign for the development of the technology. The CS efficiency for this case was more than 50%, whereas
78 most of the injected N_2 was collected, and at the final depressurization stage below hydrate stability,
79 produced gas increased from an initial 20,000 scf/day to 45,000 scf/day. This method offers significant
80 potential for efficiency and economic improvements. Direct injection of flue gas from coal-fired power
81 plant into hydrate reservoirs[36] was proposed as a potential method for reduction of the CCS cost by

eliminating the major cost of CO_2 capture. This method is mainly based on methane production by shifting the methane hydrate stability zone rather than CO_2 replacement, leading to production of methane-rich gas mixtures with up to 70% methane and storage of up to 80% CO_2 present in flue gas. Given the results, this method has a great potential to attract the industrial attention. Regarding concerns with respect to the leakage of the injected gas, it's shown that CO_2 hydrate formation could provide an additional safety factor for sealing the reservoir by forming a hydrate cap which remarkably blocks further upward gas flow[37].

Although the above investigations demonstrate that injection of CO_2-N_2 gas mixtures could provide an economically-viable method for CCS in gas hydrate reservoirs, there remains a fundamental question: How does formation of the CO_2 and CO_2-mixed hydrates (i.e., CO_2 capture) depend on the reservoir conditions after CO_2-N_2 mixtures or flue gas injection into a gas hydrate reservoir? Accordingly, experiments were conducted to investigate the efficiency of CO_2 capture during methane recovery by direct injection of flue gas at different conditions, including flue gas injection pressure, reservoir temperature, and reservoir hydrate and water saturation. This was to find out if there are specific thermodynamic conditions that are most favorable for the CCS process in hydrate-bearing sediments.

2. Experimental Section

2.1 Materials and experimental apparatus

Research grade methane with a certified purity of 99.995 vol% was purchased from BOC Limited. A synthetic flue gas composed of 85.4 mol% nitrogen and 14.6 mol% CO_2[24,36] was utilized for simulating flue gas coming from coal-fired power plants, which was provided by BOC Limited. Deionized water was obtained using ELGA DV 25 Integral Water Purification System. It is worth to note that power-plant flue gas may contain O_2, Ar, SO_2 and water beside N_2 and CO_2[38], but small amount of these gases has very minor effect on the HSZ and can be neglected[39].

Experiments were carried out using a 316 stainless steel cylindrical autoclave, a schematic of which is shown in Fig. 1. The high-pressure cell has a volume of 1700 cm^3 and a maximum working pressure of 40 MPa is surrounded by a cooling jacket. The jacket has two openings (inlet and outlet), which allows cooling fluid circulate around the cell. The cooling fluid is circulated by a cryostat (Grant LTC) to

obtain the desired temperature, ranging from 243.2 K to 303.2 K. The cell temperature was measured using a Platinum-Resistant Thermometer (PRT) coated in stainless steel with an uncertainty of 0.1 K. The Pressure was measured using a Druck pressure transducer (accuracy +/-0.05) MPa connected to top of the cell. The cell was kept vertical throughout the tests. Gas was injected from the top-cap via a high-pressure valve. A high-pressure magnetic stirrer (Top Industrie SA, France, model 6180300B) is fixed on top of the cell to faster reach of equilibrium condition by use of a stainless steel impeller, helping increase the surface contact of the components. The temperature and pressure of the system were recorded on a PC using LabView software interface (National Instruments) through a data acquisition device at regular time intervals. Gas samples were collected using high-pressure vessels. A Gas Chromatograph (GC) (Varian 3600, Agilent Technologies) was used to analyse gas samples.

2.2 Method and procedure

Injection of flue gas or CO_2-N_2 mixtures into MH reservoirs shifts hydrate stability zone (HSZ) to higher pressure at the reservoir temperature, therefore, leads to MH decomposition and CO_2-mixed hydrate formation. By comparison to the fact that MH will start decomposition as long as the thermodynamic conditions are shifted outside the HSZ, formation of CO_2 hydrate or CO_2-mixed hydrate is a complex process. This may be associated to several factors, including the composition of fluids surrounding the methane hydrate crystals, temperature/pressure conditions, the ratio of MH to the injected flue gas, and mass/heat transfer process. In porous media the methane hydrate decomposition and CO_2-mixed hydrate formation takes a long time to reach equilibrium due to mass and heat transfer process constrained by fine pores[32]. To reduce the experimental time, all experiments were conducted in bulk conditions using an autoclave with a magnetic mixer (Fig. 1). A synthetic flue gas was directly injected into MH and then the system was depressurised step by step. Once thermodynamic equilibrium was reached at each pressure stage at a set temperature, a gas sample was taken and its composition was analysed using a GC. The experiment was repeated at three different temperatures to investigate the effect of reservoir temperature. Furthermore, to understand the dependence of the CO_2 capture efficiency on the MH reservoir volume and hydrate saturation, i.e., ratio of flue gas to MH, experiments were conducted in the presence of different amounts of MH initially formed before flue gas injection. It should be noted that less water was added to the system for the experiment with a low ratio of flue gas to MH to achieve

138 the desired gas to hydrate ratio and to be able to have continuous mixing without blockage due to
139 redundant hydrate formation.
140 Fig. 2 presents the HSZs of the gas-water systems tested in this work together with the experimental
141 temperature and pressure conditions. In order to mimic the temperature of typical MH reservoirs,
142 experiments were conducted at temperature ranging from 273.2 to 283.2 K. All experiments were
143 started at a pressure below the flue gas HSZ to avoid formation of CO_2-N_2 mixed hydrates. However,
144 from a thermodynamic point of view, the possibility of CO_2-N_2-CH_4 mixture hydrate formation still
145 exists at the experimental conditions. At the experimental conditions the other possible hydrate
146 compositions are CO_2-CH_4 and N_2-CH_4 hydrates. Here, CO_2 will fill the large cavities, while N_2 will
147 enter to small cavities for thermodynamic stabilization[11,40]. The main reason for MH dissociation and
148 mixed hydrate formation is the chemical potential shift due to the change in the gas composition, but
149 CO_2/CH_4 replacement could also occur owing to higher stability of CO_2 hydrate compared to MH. It
150 should be noted that the mechanism of flue gas replacement with CH_4 is not fully understood and there
151 are controversial ideas about that.[34,41] As can be seen, in all the experiments, the staged depressurisation
152 process was stopped just above the methane hydrate decomposition pressure at the experimental
153 temperature, since injected flue gas pressure must be higher than that of existing MH reservoirs. In the
154 same line, the optimum conditions for CS can be defined as points at which the ratio of CO_2/(N_2+ CO_2)
155 (C-ratio) in hydrate phase is maximum, or consequently the C-ratio in gas phase is minimum. It
156 therefore is a key point to analyse the gas composition at each stage to determine the optimum
157 conditions for CO_2 capture.

158 The following general procedure was used for all the experiments. Deionised water was loaded in the
159 autoclave. After vacuuming, methane was injected to the desired pressure at room temperature ~293 K.
160 Then the system was set to the target temperature whilst stirring at 500 rpm to form MH. The stirrer
161 was allowed to run until equilibrium was achieved, which was indicated by a stabilised system pressure.
162 Following that, synthetic flue gas was injected to the autoclave, allowing the system to reach a pressure
163 between the MH phase boundary and flue gas hydrate phase boundary (Fig. 2). Gas samples were taken
164 and analysed at specified time intervals, usually every 24 hours. The process was continued until an

equilibrium was reached, at which no further changes in gas composition were observed. Following this, the system pressure was reduced to the next pressure stage by draining certain amount of the gas from the system after stopping the stirrer. The same procedure was repeated for each step up to the final pressure stage. The overall system composition which is made up of all gases in the water, hydrate and gas phases, were calculated using mass balance and measurement of the removed gas at end of each depressurization stage. These results can be found in supplementary materials. Table 1 shows the experimental conditions including temperature, initial water amount, system pressure after methane injection at room temperature, start pressure and end pressure of depressurization, and molar ratio of initial flue gas to CH_4 in the autoclave.

3. Results and Discussion

As with most gas injection methods, an investigation of the effects of pressure on CS through flue gas injection is necessary to determine at which pressure there is a maximum CS, for a particular MH reservoir at certain temperature. By optimizing the pressure of the injected gas and operating at such conditions close to the optimum pressure, the economics of the gas injection projects can be further improved. This knowledge is essential for field-scale applications as it is preferably based on the method efficiency. In this work pressure varied rather than temperature because it is relatively easier to control the reservoir pressure compared to the temperature. GC analysis results versus pressure were plotted as shown in Fig. 3 a-f to determine the ideal pressure for each test. This pressure is seen in Fig. 3 a-f where clear downward peaks were observed for C-ratio graphs. The initial reduction of this ratio can be justified by the fact that more CO_2 than N_2 goes to the hydrate phase (CO_2 hydrate or CO_2-mixed hydrates) due to relative thermodynamic stability of CO_2 at lower pressures and N_2 promotes CO_2-CH_4 molecule exchange by interfering CH_4 in small cages[32], which is in agreement with other published work[6]. The possible reason for the secondary increase after optimum pressure is that at lower pressures, N_2 molecules stop acting as promoting agents for CO_2 sequestration, which results in reduction in the driving force of N_2 on CH_4 hydrates. This in turn, will possibly lead to destabilization of those excess CO_2 hydrates, which were stabilized by N_2. Furthermore, sharper increase in the C-ratio at the final depressurization stage just above CH_4 hydrate dissociation pressure indicates some of CO_2-mixed

hydrates were dissociated significantly above the CO_2 HSZ, assuming that there is no possibility of N_2 mixed hydrate formation at this condition. It should be noted that C-ratio changes were sharper against pressure at lower temperatures and with higher MH saturation compared to those at higher temperatures and with lower MH saturation, respectively, indicating the higher chemical potential shift at former conditions compared to latter ones after flue gas injection. Accordingly, the trend of changes in the C-ratio for the gas phase shows that the occupancy ratio of large to small cages during CO_2 mixed hydrate formation changes with pressure. What's more, the experiments were conducted with two different amounts of initially formed MH to clarify the effect of hydrate saturation in the reservoir. Fig. 3 indicates that at all temperatures, C-ratio decreased with increasing initial MH and water content, which can be attributed to CO_2-CH_4 replacement, and higher solubility of CO_2 compared to N_2. More CS through more MH can be considered as further support for CO_2-CH_4 replacement without full dissociation of hydrate structure, which is in agreement with another work[34]. However, further investigation is required for full understanding of the mechanism. As illustrated in Fig. 3a-f, CH_4 graphs showed upward trends. Corresponding to the increase in CH_4 concentration in the gas phase, graphs for N_2 concentration showed continuous downward trends. Meanwhile, CO_2 concentration slightly increased after the initial reduction. This is continued until the end of the tests which can be explained using the same reason for the increase in the C-ratio. It is clear from the aforementioned graphs that CH_4 percent in the gas phase increased with both reduction in the temperature and an increase in the amount of initially formed MH. Accordingly, more favourable conditions for CS are also more favourable for methane recovery. These results suggest that chemical shift method is able to efficiently recover CH_4 and facilitate the CH_4 transport from the hydrate phase to the gas phase.

Fig. 4 and Table 2 show measured properties of the system at optimum conditions for all experiments. As shown in Fig. 4-a, the C-ratio in the gas phase for the optimum pressure greatly increases with increase in the temperature, whereas there is no significant difference in this ratio for total system composition (see Fig. 4-b), which is reasonable as system compositions at start of experiments were equal and removed gas doesn't have a significant effect. This suggests that the lower temperatures favour more CO_2 than N_2 in the hydrate phase. Furthermore, at the optimum pressure, the C-ratio in the gas phase is lower for the systems with more MH, while this ratio for overall system composition is

higher for the systems with more MH than those with less MH. This can be attributed to the fact that the more MH and water have more capacity of storing CO_2. For each component in the system at each depressurization step, the total concentration will increase if the concentration of the component in the gas phase is less than that of the total composition, otherwise it will decrease. With this in mind, it is worth noting that, as shown in Fig. 4 b, the overall C-ratio in the system was almost the same for experiments with the same amount of initial methane. However the ratio is lower for the experiments with lower initial MH owing to less increase of CH_4 in the gas phase during the initial steps compared to that of higher initial MH that results from less driving force through chemical potential shift. By comparing the slopes of CH_4 concentration in Fig. 4-a, the temperature effect on CH_4 recovery for higher initial MH saturation is relatively higher than that with less MH at optimum conditions. However, the slope for the C-ratio was almost the same for both amounts of initial MH. This effect is possibly derived from higher concentrations of overall N_2 at lower MH concentrations and also higher temperatures (see Fig. 4-b), reducing the temperature effect by interfering MH at small pores without replacing with them. For overall system CH_4 at the optimum conditions, the concentration at higher temperatures is less than that at lower temperature. This could be plausibly justified by the fact that upon high pressure at start of the experiments at high temperature, relatively more flue gas was injected which, in turn, kept the total CH_4 concentration at lower state. In contrast, for the same reason, fractions of CO_2 and N_2 increase with temperature.

To depressurise the system some gas mixture had to be drained out from the system. This in turn will lead to a change in the system composition. Accordingly, because the system composition was changing during the depressurisation process, there was a need to define a parameter to eliminate the effect of these changes. Thus, “repartition” ratio, R is defined as the C-ratio in the gas phase divided by that in the overall system. This is to examine whether the apparent optimum in the current method is the true optimum. The R-values for each step in all experiments were calculated and are plotted in Fig. 5, in which the minimum R-value at each test is the indication of the optimum point. The resulting optimum conditions from R-values for all experiments, as can be seen, were the same as those determined based

on the gas composition of the existing system. Therefore, it can be concluded that optimum conditions can be determined by analysis of the gas composition after some gas was removed.

Fig. 6 illustrates the optimum pressure for each experiment together with the predicted HSZs for CH_4-flue gas mixtures with different mole ratios of CH_4. As can be seen, all optimum conditions are in a pressure range between the HSZs of 30 mol% and 50 mole% methane, approaching the HSZs with 30 mol% methane as the initial MH decreases and approaching to the HSZs with 50 mol% methane as the initial MH increases. Furthermore, in terms of pressure, the two optimum CO_2 capture pressures are closer at lower temperature compared with those at higher temperatures. However, there are larger differences in C-ratio with change of pressure at lower temperature compared with higher temperatures (see Fig.3). By taking the above two reasons into account, it can be concluded that the pressure effect on CO_2 capture efficiency is more significant at lower temperatures than at higher temperatures.

While the field of CS at MH reservoirs is in its infancy, we believe that enhancing the technologies at a conceptual process level is crucial to help evolve the realistic viability of the proposed methane recovery method and identifying the critical influencing parameters that must be considered to make a future field application more successful. Importantly, through our experiments and analysis, we have identified the optimum conditions and key parameters for improving the overall economic feasibility of the CS at MH reservoirs. By taking all above results into account, we suggest a simple field trial plan to both capture CO_2 and recover methane by continuous injection of flue gas into a gas hydrate deposit, in which reservoir pressure can be controlled and adjusted to near optimum pressure according to temperature change and MH saturation reduction. This can be implemented through different scenarios, for example, one injection well and one production well, or one injection well and multiple production wells, or one well for both injection and production through a puff & huff process. In this regard, for reaching our goal of economic and sustainable CS and energy recovery, concerted collaborative effort among researchers from different fields will be required to facilitate flue gas process and transfer through pipelines after emission from the power plants, to determine the optimum well locations and injection/production rate, to understand more about the geological impact of the current method, and also to recognize the possible side effect that may happen to the environment.

Acknowledgments

This work was financially supported by the Skolkovo Institute of Science and Technology, Russia, which is gratefully acknowledged. The authors would like to thank Dr. Rod Burgass for his valuable contributions to the project.

References

(1) Sloan, E. D. *Nature* **2003**, *426* (November), 353.
(2) Kvenvolden, K. A.; McMenamin, M. A. **1980**.
(3) Kvenvolden, K. A.; Lorenson, T. D. American Geophysical Union, 2013; pp 3–18.
(4) Holder, G. D.; Kamath, V. A. *J. Chem. Thermodyn.* **1984**, *16* (4), 399–400.
(5) Onyango, P.; Jiang, S.; Uejima, H.; Shamblott, M. J.; Gearhart, J. D.; Cui, H.; Feinberg, A. P. *Proc. Natl. Acad. Sci. U. S. A.* **2002**, *1699* (10), 10599–10604.
(6) Park, Y.; Kim, D.-Y.; Lee, J.-W.; Huh, D.-G.; Park, K.-P.; Lee, J.; Lee, H. *Proc. Natl. Acad. Sci. U. S. A.* **2006**, *103* (34), 12690–12694.
(7) Ersland, G.; Husebø, J.; Graue, A.; Kvamme, B. *Energy Procedia* **2009**, *1* (1), 3477–3484.
(8) IPCC. *Weather* **2001**, *57*, 267–269.
(9) Dti, U. K. *Dep. Trade Ind. C.* **2007**.
(10) MacDowell, N.; Florin, N.; Buchard, A.; Hallett, J.; Galindo, A.; Jackson, G.; Adjiman, C. S.; Williams, C. K.; Shah, N.; Fennell, P. *Energy Environ. Sci.* **2010**, *3* (11), 1645–1669.
(11) Dornan, P.; Alavi, S.; Woo, T. K. *J. Chem. Phys.* **2007**, *127* (12), 124510–124700.
(12) Deusner, C.; Bigalke, N.; Kossel, E.; Haeckel, M. *Energies* **2012**, *5* (12), 2112–2140.
(13) Seo, Y.-T.; Moudrakovski, I. L.; Ripmeester, J. A.; Lee, J.; Lee, H. *Environ. Sci. Technol.* **2005**, *39* (7), 2315–2319.
(14) Yuan, Q.; Sun, C.-Y.; Liu, B.; Wang, X.; Ma, Z.-W.; Ma, Q.-L.; Yang, L.-Y.; Chen, G.-J.; Li, Q.-P.; Li, S. *Energy Convers. Manag.* **2013**, *67*, 257–264.
(15) Ota, M.; Morohashi, K.; Abe, Y.; Watanabe, M.; Smith, Jr., R. L.; Inomata, H. *Energy Convers. Manag.* **2005**, *46* (11), 1680–1691.
(16) Ota, M.; Abe, Y.; Watanabe, M.; Smith, R. L.; Inomata, H. *Fluid Phase Equilib.* **2005**, *228*, 553–559.
(17) Lee, S.; Lee, Y.; Lee, J.; Lee, H.; Seo, Y. *Environ. Sci. Technol.* **2013**, *47* (22), 13184–13190.
(18) Ersland, G.; Husebø, J.; Graue, A.; Baldwin, B. A.; Howard, J.; Stevens, J. *Chem. Eng. J.* **2010**, *158* (1), 25–31.
(19) Zhang, L.; Yang, L.; Wang, J.; Zhao, J.; Dong, H.; Yang, M.; Liu, Y.; Song, Y. *Chem. Eng. J.* **2017**, *308*, 40–49.
(20) Lee, H.; Seo, Y.; Seo, Y.-T.; Moudrakovski, I. L.; Ripmeester, J. A. *Angew. Chemie Int. Ed.* **2003**, *42* (41), 5048–5051.
(21) Goel, N. *J. Pet. Sci. Eng.* **2006**, *51* (3), 169–184.
(22) Ma, Z. W.; Zhang, P.; Bao, H. S.; Deng, S. *Renew. Sustain. Energy Rev.* **2016**, *53*, 1273–1302.
(23) Gough, C.; Mander, S.; Haszeldine, S. *Int. J. Greenh. Gas Control* **2010**, *4* (1), 1–12.
(24) Change, W. G. I. of the I. P. on C.; Metz, B.; Davidson, O.; Coninck, H. de; Loos, M.; Meyer, L. Cambridge University Press.
(25) Damen, K.; Troost, M. van; Faaij, A.; Turkenburg, W. *Prog. Energy Combust. Sci.* **2006**, *32* (2), 215–246.
(26) Feron, P. H. M.; Hendriks, C. A. *Oil Gas Sci. Technol.* **2005**, *60* (3), 451–459.
(27) Enterprise, S. *Scottish Enterp. Glas.* **2011**.
(28) Hendriks, C. A.; Blok, K.; Turkenburg, W. C. In *Climate and Energy: The Feasibility of Controlling CO2 Emissions*; Springer Netherlands: Dordrecht, 1989; pp 125–142.
(29) Peeters, A. N. M.; Faaij, A. P. C.; Turkenburg, W. C. *Int. J. Greenh. Gas Control* **2007**, *1* (4), 396–417.
(30) Pires, J. C. M.; Martins, F. G.; Alvim-Ferraz, M. C. M.; Simões, M. *Chem. Eng. Res. Des.*

2011, *89* (9), 1446–1460.
(31) Boot-Handford, M. E.; Abanades, J. C.; Anthony, E. J.; Blunt, M. J.; Brandani, S.; Mac Dowell, N.; Fernández, J. R.; Ferrari, M.-C.; Gross, R.; Hallett, J. P. *Energy Environ. Sci.* **2014**, *7* (1), 130–189.
(32) Shin, K.; Park, Y.; Cha, M.; Park, K.-P.; Huh, D.-G.; Lee, J.; Kim, S.-J.; Lee, H. *Energy & Fuels* **2008**, *22* (5), 3160–3163.
(33) Koh, D.; Kang, H.; Kim, D.; Park, J.; Cha, M.; Lee, H. *ChemSusChem* **2012**, *5* (8), 1443–1448.
(34) Cha, M.; Shin, K.; Lee, H.; Moudrakovski, I. L.; Ripmeester, J. A.; Seo, Y. *Environ. Sci. Technol.* **2015**, *49* (3), 1964–1971.
(35) Schoderbek, D.; Martin, K. L.; Howard, J.; Silpngarmlert, S.; Hester, K. In *OTC Arctic Technology Conference*; Offshore Technology Conference, 2012.
(36) Yang, J.; Okwananke, A.; Tohidi, B.; Chuvilin, E.; Maerle, K.; Istomin, V.; Bukhanov, B.; Cheremisin, A. *Energy Convers. Manag.* **2017**, *136*, 431–438.
(37) Tohidi, B.; Yang, J.; Salehabadi, M.; Anderson, R.; Chapoy, A. *Environ. Sci. Technol.* **2010**, *44* (4), 1509–1514.
(38) Ziabakhsh-Ganji, Z.; Kooi, H. *Appl. Energy* **2014**, *135*, 43–52.
(39) Chapoy, A.; Nazeri, M.; Kapateh, M.; Burgass, R.; Coquelet, C.; Tohidi, B. *Int. J. Greenh. Gas Control* **2013**, *19*, 92–100.
(40) Kvamme, B.; Iden, E.; Tveit, J.; Veland, V.; Zarifi, M.; Qorbani, K. *J. Chem. Eng. Data* **2017**, *62* (5), 1645–1658.
(41) Bai, D.; Zhang, X.; Chen, G.; Wang, W. *Energy Environ. Sci.* **2012**, *5* (5), 7033.

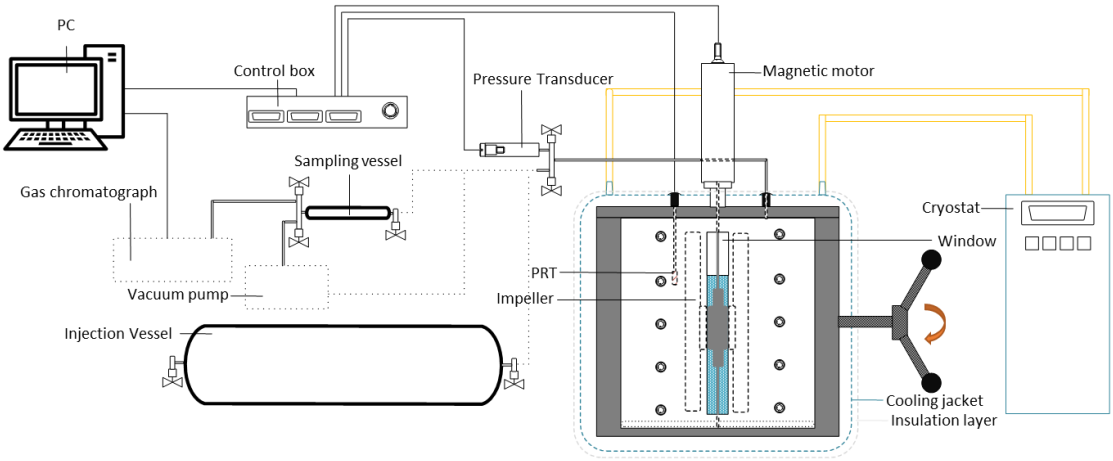

Fig. 1 Schematic of the high pressure autoclave

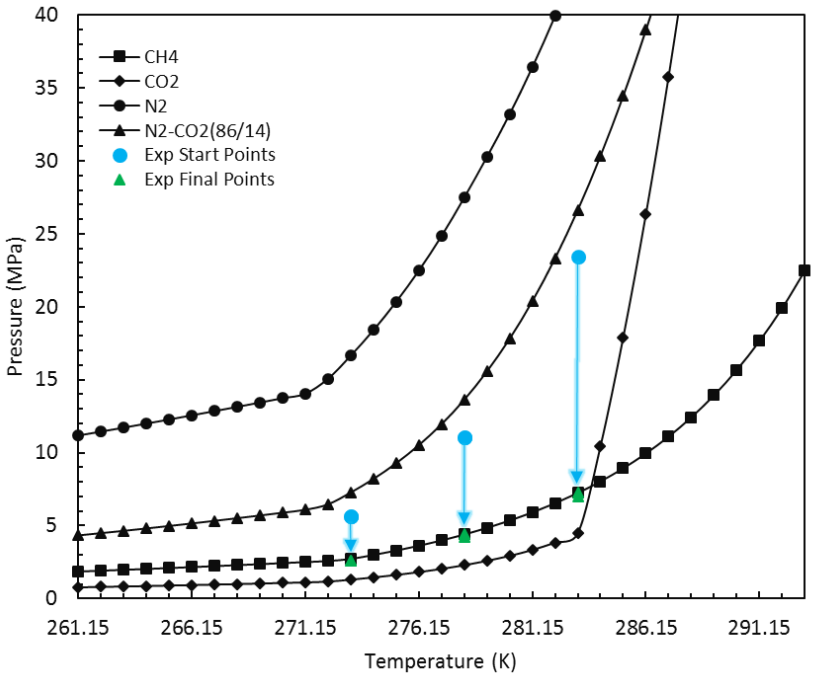

385

386 Fig. 2 The predicted hydrate stability zones of CH_4, CO_2, N_2, flue gas, and the experimental conditions

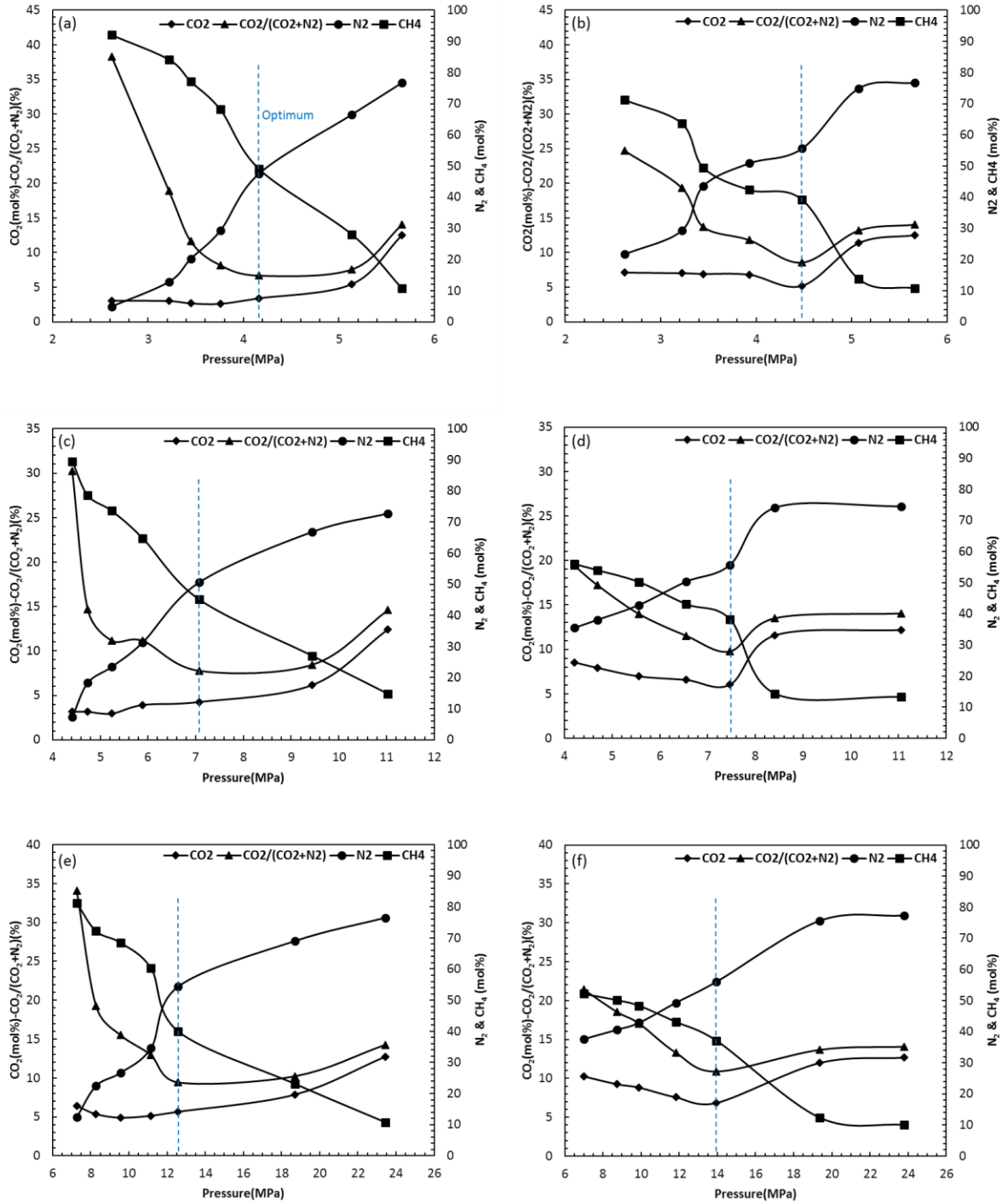

387

388 Fig. 3 Variation in the gas composition change during the stepwise depressurization. (a)-(f) for

389 Experiments 1-6.

390

391

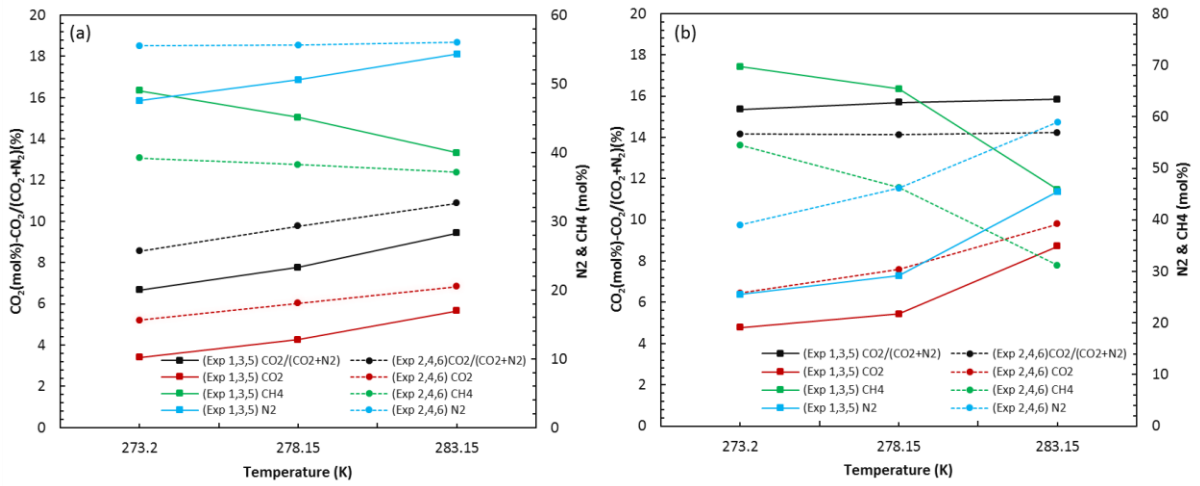

Fig. 4 (a) The measured gas composition and (b) total composition at optimum conditions for all experiments.

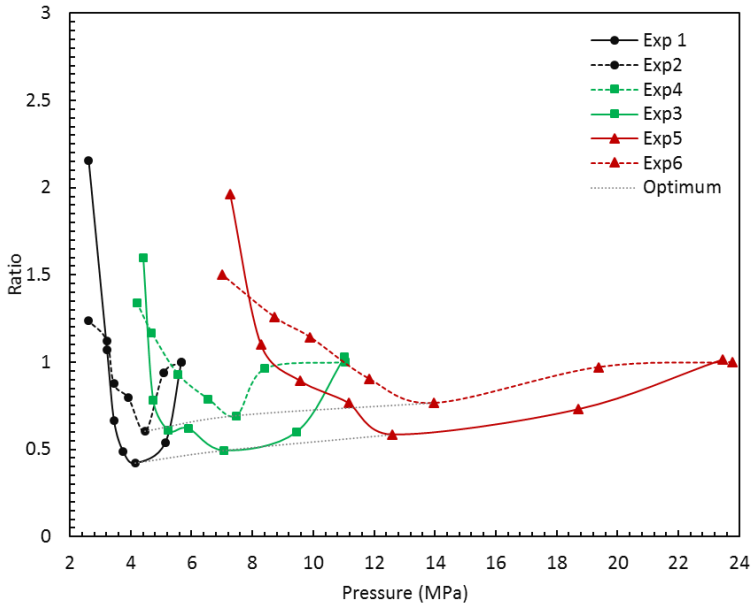

Fig. 5 R-Values variation with the system pressure at the experimental temperatures

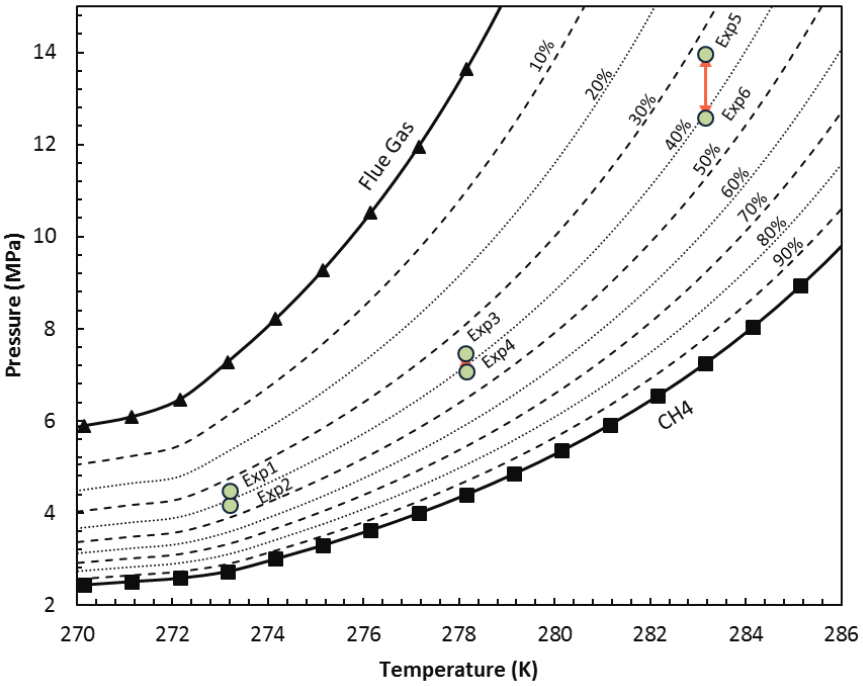

Fig. 6 Location of the determined optimum conditions for CO_2 capture for different gas hydrate reservoir conditions

Table 1 Experimental conditions

Exp.	T (K)	Water (g)	CH_4 injection P (MPa)	Start P (MPa)	End P (MPa)	Initial flue gas to CH_4 ratio(mol/mol)
1	273.2	1150	17.58	5.66	2.62	0.59
2	273.2	500	7.03	5.66	2.62	1.04
3	278.2	1150	19.31	11.03	4.41	0.82
4	278.2	500	8.62	11.05	4.21	1.62
5	283.2	1150	22.06	23.44	7.27	1.91
6	283.2	500	11.38	23.79	6.99	3.17

Table 2 The determined optimum conditions for CO_2 capture as hydrates

Exp.	Pressure (MPa)	Gas phase composition				Overall composition			
		N_2 (mol%)	CH_4 (mol%)	CO_2 (mol%)	$CO_2/(CO_2+N_2)$	N_2 (mol%)	CH_4 (mol%)	CO_2 (mol%)	$CO_2/(CO_2+N_2)$
1	4.16	47.60	49.00	3.40	6.67	25.49	69.74	4.77	15.36
2	4.48	55.60	39.20	5.20	8.55	39.07	54.49	6.44	14.15
3	7.07	50.62	45.12	4.26	7.76	29.19	65.38	5.43	15.69
4	7.46	55.70	38.27	6.03	9.78	46.14	46.27	7.59	14.12
5	12.58	54.38	39.96	5.66	9.43	45.46	45.82	8.72	15.84
6	13.95	56.04	37.12	6.84	10.88	59.01	31.20	9.79	14.23